DEGREE PROJECT IN ELECTRICAL ENGINEERING,
SECOND CYCLE, 30 CREDITS
STOCKHOLM, SWEDEN 2018

Study of the effects of applying higher symmetries to printed filters

JOSE LUIS MEDRÁN DEL RÍO

KTH ROYAL INSTITUTE OF TECHNOLOGY
SCHOOL OF ELECTRICAL ENGINEERING AND COMPUTER SCIENCE

Study of the effects of applying higher symmetries to printed filters.

JOSE LUIS MEDRÁN DEL RÍO

Degree Project in Electrotechnical Theory and Design
Date: June 14, 2018
Supervisor: Qingbi Liao
Examiner: Oscar Quevedo-Teruel
Swedish title: Studie av högre symmetries effekt på tryckta filter
School of Electrical Engineering and Computer Science

Study of the effects of applying higher symmetries to printed filters

Jose Luis Medrán del Río

Abstract

In recent years, a new field of study has arisen around the application of the so-called higher symmetries to structures that were already thought to be completely studied and with no room for improvement in terms of benefits.

There are two types of higher symmetries, named glide and twist symmetries. The objective of this Master thesis is the study of the effects coming from the application of the glide symmetry on a printed filter in microstrip technology and its comparison with a filter with conventional reflective symmetry.

The filter was adapted to the glide characteristics and we provide its behavior from different points of view with the purpose of reaching a better understanding of the consequences of applying the glide symmetry on this type of printed filters.

Three prototypes were manufactured and measured to validate the simulated results.

Keywords: Glide symmetry, printed filter, microstrip, higher symmetries.

Studie av högre symmetries effekt på tryckta filter

Jose Luis Medrán del Río

Abstrakt

Under senare år har ett nytt forskningsfält uppkommit genom applikationen av högre symmetrier till strukturer som redan studerats extensivt.

Det finns två typer av högre symmetrier och dessa kallas glid- och vridsymmetrier. Målet med detta masterexamensarbete är att studera effekten som kommer från applikationen av glidsymmetri på ett filter, implementerat i mikrostripsteknik. Jämförelse med filtret med enbart reflektionssymmetri görs också.

Glidsymmetri har introducerats i filtret och vi undersöker filtrets beteende från en rad olika synvinklar för att uppnå en bättre förståelse för konsekvenserna av glidsymmetri för den här typen av tryckta (”printed”) filter.

Flera prototyper har tillverkats och mätts för att validera de simulerade resultaten.

Nyckelord: Glidsymmetri, tryckta filter, mikrostrip, högre symmetrier.

Estudio de los efectos de aplicar simetrías superiores a filtros impresos

Jose Luis Medrán del Río

Resumen

En los últimos años ha surgido un nuevo campo de estudio entorno a la aplicación de las llamadas simetrías superiores a estructuras que ya se pensaban completamente estudiadas y sin margen de mejora en cuanto a prestaciones.

Hay dos tipos de simetrías superiores, denominadas simetría glide y simetría twist. El objetivo de esta tesis de Máster consiste en el estudio de los efectos provenientes de la aplicación de la simetría glide sobre un filtro impreso en microstrip y su comparación con un filtro con simetría reflectiva convencional.

El filtro se ha adaptado a las características glide y proporcionamos su comportamiento desde diferentes puntos de vista con el fin de llegar a una mejor comprensión de las consecuencias de aplicar la simetría glide en este tipo de filtros impresos.

Tres prototipos han sido manufacturados y medidos para validar los resultados simulados.

Palabras clave: Simetría glide, filtro impreso, microstrip, simetrías superiores.

Estudi dels efectes d'aplicar simetries superiors a filtres impresos

Jose Luis Medrán del Río

Resum

En els últims anys ha aparegut un nou camp d'estudi al voltant de l'aplicació de les cridades simetries superiors a estructures que ja es pensaven completament estudiades i sense marge de millora pel que fa a prestacions.

Hi ha dos tipus de simetries superiors, denominades simetria glide i simetria twist. L'objectiu d'aquesta tesi de Màster consisteix en l'estudi dels efectes provinents de l'aplicació de la simetria glide sobre un filtre imprès en microstrip i la seva comparació amb un filtre amb simetria reflectiva convencional.

El filtre s'ha adaptat a les característiques glide i proporcionem el seu comportament des de diferents punts de vista per tal d'arribar a una millor comprensió de les conseqüències d'aplicar la simetria glide en aquest tipus de filtres impresos.

Tres prototips han sigut manufacturats i mesurats per validar els resultats simulats.

Paraules clau: Simetria glide, filtre imprès, microstrip, simetries superiors.

Acknowledgments

I would like first to thank Oscar Quevedo-Teruel of the Department of Electromagnetic Engineering on the School of Electrical Engineering and Computer Science at KTH Royal Institute of Technology. The door to Dr. Quevedo-Teruel's office was always open whenever I ran into a trouble spot or had a question about my research or writing. He consistently allowed this paper to be my own work but steered me in the right direction whenever he thought I needed it.

I would like to thank my supervisor, Qingbi Liao, PhD student of the Department of Electromagnetic Engineering on the School of Electrical Engineering and Computer Science at KTH Royal Institute of Technology, for agreeing to be my thesis advisor and for the help offered during the development of this thesis.

I would also like to thank Dr. Francisco Medina-Mena and Dr. Armando Fernández Prieto from the Microwaves Group at University of Seville. Theirs was the starting point for this project and without their help and support it would have been much more difficult to achieve these results. Dr. Armando also offered himself to manufacture the prototypes for this thesis, so I'm very grateful to him.

I would also like to thank KTH Royal Institute of Technology and Politechnic University of Valencia as entities, as well as the Erasmus+ Program, since they have offered me the opportunity to increase my knowledge not only on theoretical and practical matters related to my studies, but also to let me grow as a person, having the opportunity to live in another environment with new challenges that I have been able to overcome, letting me know myself better and improving my capabilities.

Of course, my friends have been an important support for me in this new adventure, so I want to thank them for being with me, the ones I knew before arriving at Stockholm and the new ones whom I have met here.

To the people at the master's thesis room at Teknikringen 33, especially to David, Alberto, Oskar and Neelu. Thanks to them the workplace was a better place and they helped me whenever I needed it.

Y por supuesto, quisiera dar las gracias a mis padres, quienes me han dado todo en esta vida y gracias a ellos estoy hoy aquí, después de tantos años de trabajo, terminando esta tesis. Su fortaleza, sacrificio y ayuda han sido indispensables para que yo sea la persona que soy hoy y a ellos se lo debo todo.

Gracias **Thank you** **Tack**

Contents

Chapter 1: Introduction

This master thesis has as main objective the study of the effects of applying higher symmetries (in this case, glide symmetry) to a previously design that uses regular reflective symmetry. In order to accomplish this goal, we are going to follow the next scheme.

In the first place, we will replicate and explain the results obtained in [1] in order to completely understand the starting structure so we can explain the results that we will obtain after applying the glide symmetry.

Afterwards, we will explain in detail what are these high symmetries using several publications as examples to deduct the effects that are going to occur to our original structure.

Then, we will exhaustively study the new structure, applying the glide symmetry in different ways so we can fully understand the behavior of our structure.

The next step will be compare the results between the structure presented in [1] and the new ones, so we can see the effects of the glide symmetry over this kind of structures. Also, three prototypes have been manufactured in order to validate the results obtained in the simulations.

Finally, we will provide some conclusions over this master thesis and explain the environmental impact that has the applications and devices that include these kinds of elements.

Before we start digging into the project itself, we are going to show the timeline followed in this thesis.

1.1 Timeline

In the table 1.1 we can see the periods dedicated to each stage of the master thesis.

Stage / Period	February 2018				March 2018				April 2018				May 2018				June 2018			
Getting used to CST	X	X	X	X																
Study references			X	X	X															
Study original structure				X	X	X	X	X	X											
Applying changes										X	X	X	X	X						
Study those changes										X	X	X	X	X	X					
Redact thesis												X	X	X	X	X	X	X		
Manufacture prototypes																X	X			

Table 1.1. Timeline of the thesis.

Chapter 2: Original design

2.1 Structure

The original structure under study is a low-pass filter for the common mode that behaves as an all-pass filter for the differential mode. This behavior is achieved by employing a periodic microstrip differential line.

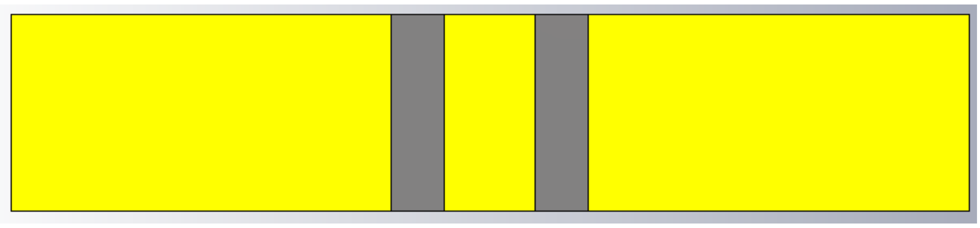

Figure 2.1. Top view of the filter.

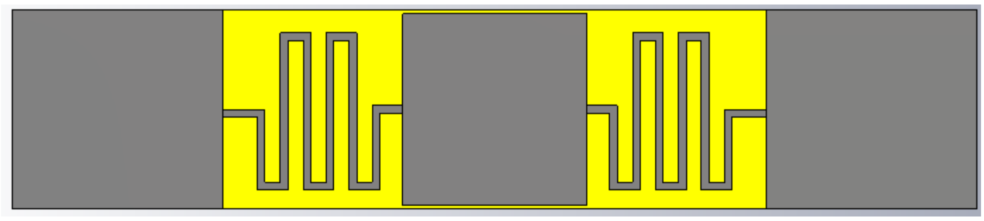

Figure 2.2. Bottom view of the filter.

First of all, we need to understand why it is so important the use of the differential signaling instead of single-ended signaling.

Single-ended signaling [2] is a simple and common way of transmitting an electrical signal from a sender to a receiver. One wire carries a varying voltage that represents the signal, while the other wire is connected to a reference voltage, usually ground. The current associated with the signal travels from sender to receiver and returns to the power supply through the ground connection. The number of wires required in the circuit will depend on the number of signals plus one shared ground connection.

Unlike single-ended signals, differential signaling makes use of two complementary signals in order to transmit one information signal. So, one information signal requires a pair of conductors; one carries the signal and the other carries the inverted signal. Usually, these voltage signals are balanced, so both amplitudes are equal and of opposite sign.

The information is retrieved in the receiver by detecting the potential difference between the inverted and non-inverted signals. And by analyzing this dual signal and its voltage difference the receiver can understand whether the signal is transmitting a 1 or a 0, or a high or low voltage.

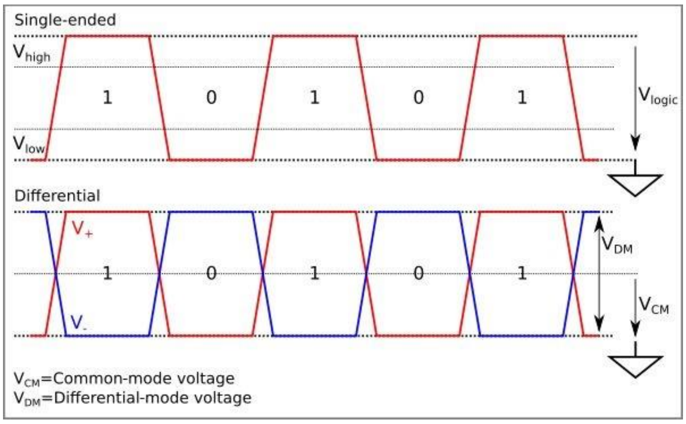

Figure 2.3. Single vs Differential signaling [2].

So, for now we know that differential signaling takes more space in the PCB since for each transmitted signal, two conductors are needed. But there are several advantages that makes differential signaling so appealing to high speed design applications [2,3], such as:

1. No return current. Since differential signals are equal and opposite, they do not necessarily send a return signal to ground and the ground reference becomes less important.
2. Resistance to incoming Electromagnetic Interference (EMI) and Crosstalk. Differential signaling has the benefit of reducing any incoming electromagnetic interference or crosstalk introduced from outside the conductors. Since it is equally distributed between the inverted and non-inverted

signal, any change in amplitude that external EMI issues can cause is reduced.

3. Reduction of Outgoing EMI and Crosstalk. Differential signaling will also generate their own EMI while transmitting information, just like single-ended signals. But the two signals in a differential pair will create electromagnetic fields that are (ideally) equal in magnitude but opposite in polarity which will effectively cancel out any EMI emissions.
4. Lower voltage operation. Differential signals can operate at lower voltages than single-ended signals, all while maintaining the signal-to-noise ratio (SNR). Also, the use of lower voltage brings some benefits as being able to use lower supply voltages, reduced power consumption and reduced EMI emissions.
5. Precise timing. Single-ended signals make use of a lot of factors in order to determine what kind of logic state they might be in (power supply voltage, threshold characteristics, reference voltage, variations and tolerances). Instead, with differential signals is much more straightforward and precise to determine the logic state since only the potential differential is used for the decision.

So, now we understand why we want to use differential signaling in our high-speed digital circuits, but in any differential signal transmission method there also exist some level of common-mode noise (mainly caused by amplitude unbalance and time skew). This presence of common-mode may worsen the specifications of our devices since it can introduce undesired radiation and electromagnetic interferences.

This way, the design of differential devices with high common-mode rejection has become one important field of study in the last years in order to achieve the better results possible in terms of performance of high-speed circuitry.

Traditionally, in the MHz domain, common-mode chokes have been used to suppress common-mode propagation, sadly, this strategy does not work in the GHz domain. Several methods have been proposed to account for this matter like we can see in [4,5,6,7]. Nevertheless, we are going to focus, as mentioned before, in the solution presented in [1].

The idea of making a low pass-filter for the common mode is also important since there are a lot of devices, such as, dual-band and multiband components which are inherently bad at common-mode rejection. Also, these kinds of components are very used in wireless communications and in new technologies like Internet of Things so the need for a component or device which acts as a pre-stage for the task of rejecting the common-mode is a very important issue nowadays.

The structure under study, as seen in Figure 1, is composed of a pair of coupled microstrip lines loaded with a periodic distribution of centered conductor patches. The patches are symmetrically series connected to the ground plane by means of narrow (high impedance) strip lines. These lines behave as inductors in the frequency range of interest. Under common-mode operation, the pattern printed in the ground plane in conjunction with the coupled lines of the top side behaves as a low-pass filter.

Hence, we obtain a very nice device with broadband behavior which rejects the common-mode but let pass the differential-mode. This structure can be used as a pre-stage, as already mentioned, before components with intrinsic poor common-mode rejection.

2.2 Analysis of the original structure

In order to fully understand the structure, we have performed several simulations with the software CST MICROWAVE STUDIO. The detailed results will be explained and discussed in this section of the report.

In the first place, let’s remember the structure which will be simulated. In the figures 2.4 and 2.5 we can completely observe the diverse measures for each element of the structure. In the next sections where we modify this structure we won’t see these measures again since all the dimensions will be kept.

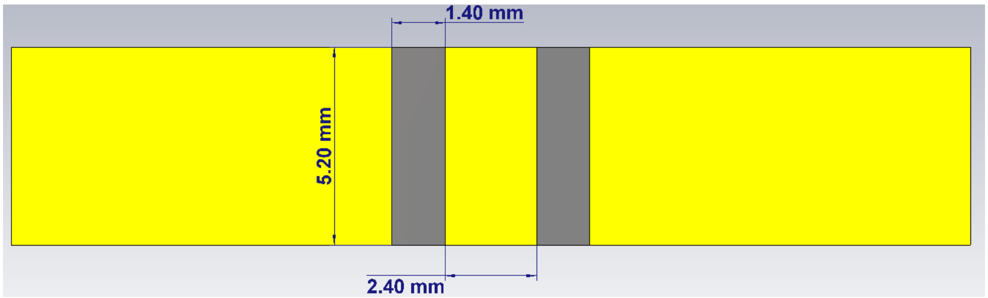

Figure 2.4. Dimensions of the structure's top.

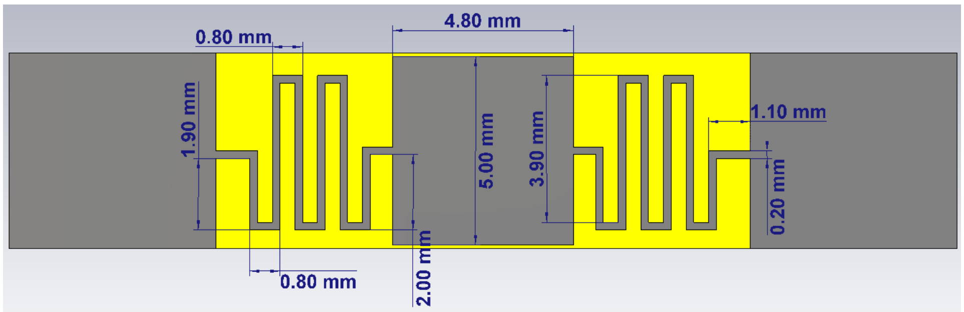

Figure 2.5. Dimensions of the structure's bottom.

This is the representation of one unit cell. In this section we will study several compositions from this unit cell. Specifically, we will explore the behavior of the structure with 1, 2 and 4 cells in order to understand the implications that come from stack several unit cells to the final performance.

For the purpose of fully understand the behavior of the structure we will focus on the two modes that have significant value to us, the common mode, also known as the even mode, and the differential mode or odd mode.

Before we start showing the results and discussing them, we would like to note first the simulation conditions in order to present all the needed data for achieving these results, so people will be able to corroborate them.

Like we have mentioned before, the simulations have been done in CST MICROWAVE STUDIO, specifically, in the 2018 version. As for the materials used in this study, we have used PEC as the material for the lines and ground plane in order to not increase too much the simulation time, since the results are practically the same as using copper. And for the substrate we have used Arlon CuClad 250LX, the characteristics of this substrate are: $\varepsilon_r = 2.43$ and $height = 0.49\ mm$, we have used the lossless version.

For simulating the structure, waveguide ports have been used in order to obtain a view of all the modes of interest that propagate through the structure. The main issue at the time of setting the port is that we have to make the waveguide port large enough that all the energy in the EM fields around the line are captured so that the port impedance can be calculated correctly, but not so large that the truncated field solution becomes overmoded or inaccurately-meshed. There is no exact rule to follow, but we can use the following approximation, which can be modified in case of need.

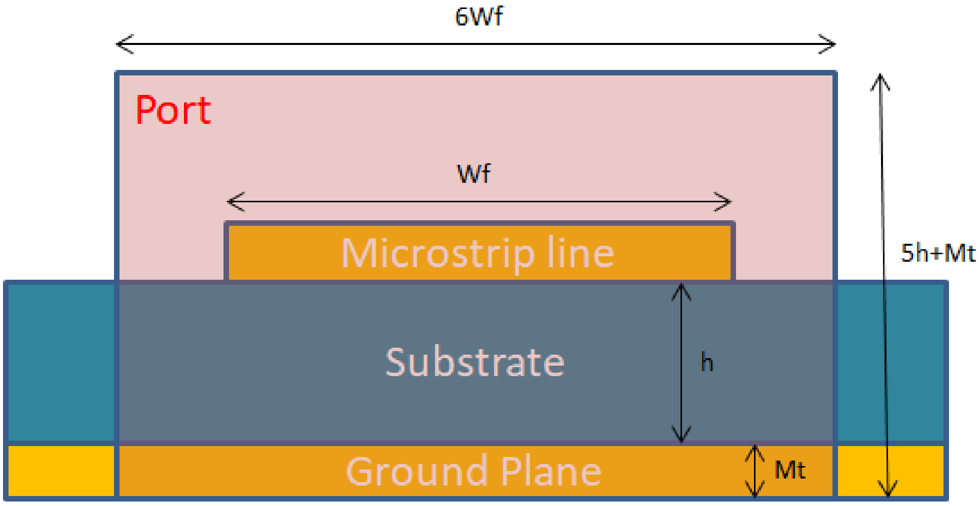

Figure 2.6. Port set-up.

So, after this introduction we will proceed to show the results obtained from the original structure.

Firstly, we will show the electromagnetic fields on the ports in order to show both modes. After that, we will focus on other parameters like the S-parameters and the dispersion diagram, so we are able to comprehend the structure.

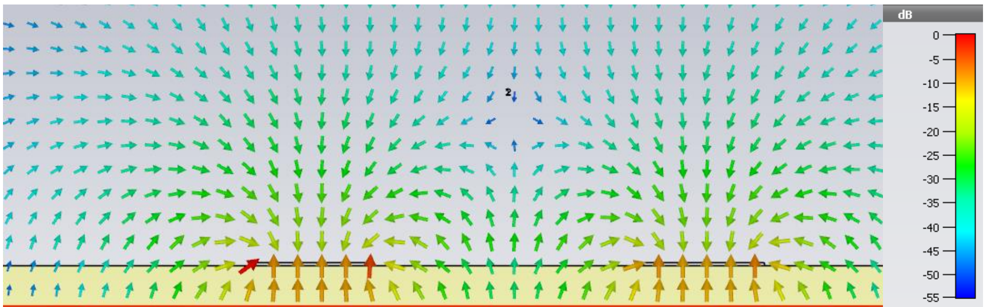

Figure 2.7. Common Mode (e-field) of the structure.

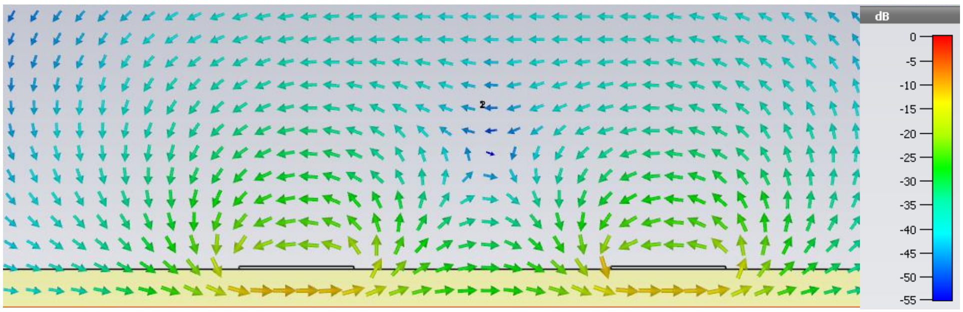

Figure 2.8. Common Mode (h-field) of the structure.

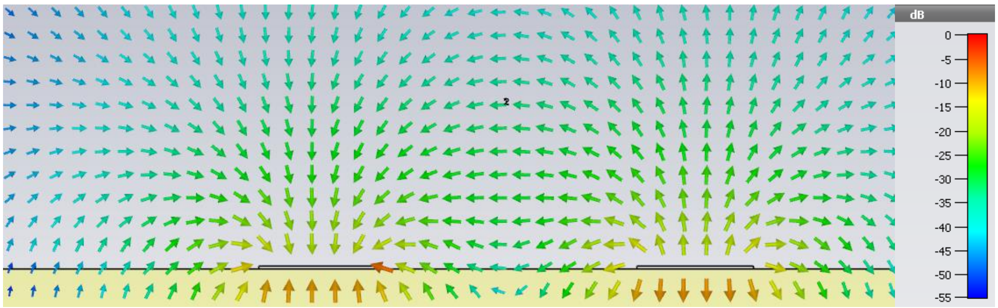

Figure 2.9. Differential Mode (e-field) of the structure.

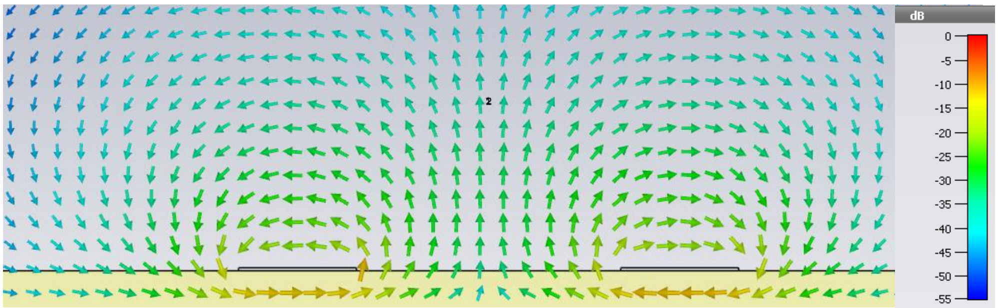

Figure 2.10. Differential Mode (h-field) of the structure.

In the figures 2.7-2.10 we observe the two modes of interest on the port 1; in the case of the port 2, the results are practically equal.

We have already discussed the importance of the differential mode in communications given its advantages over the common mode. So now we are going to see how this structure achieves the goal of rejecting the common mode without interfering too much with the differential mode.

In order to see the performance of this structure we will focus on the S-parameters and the dispersion diagram.

So now, in the figures 2.11-2.14 we are able to observe these parameters.

First, we will compare the S-parameters for each number of cells and modes in order to have a more complete view about the performance of the filter and to have a better understanding about the fact of using multiple cells.

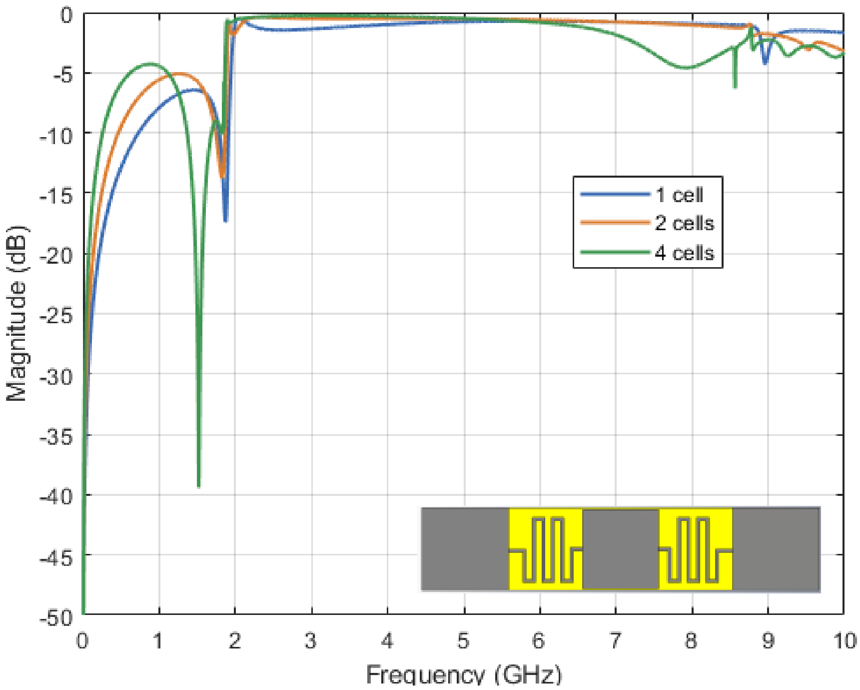

Figure 2.11. S_{11} parameter for the common mode for the structure descripted in Figures 2.4 and 2.5 for 1, 2 and 4 cells.

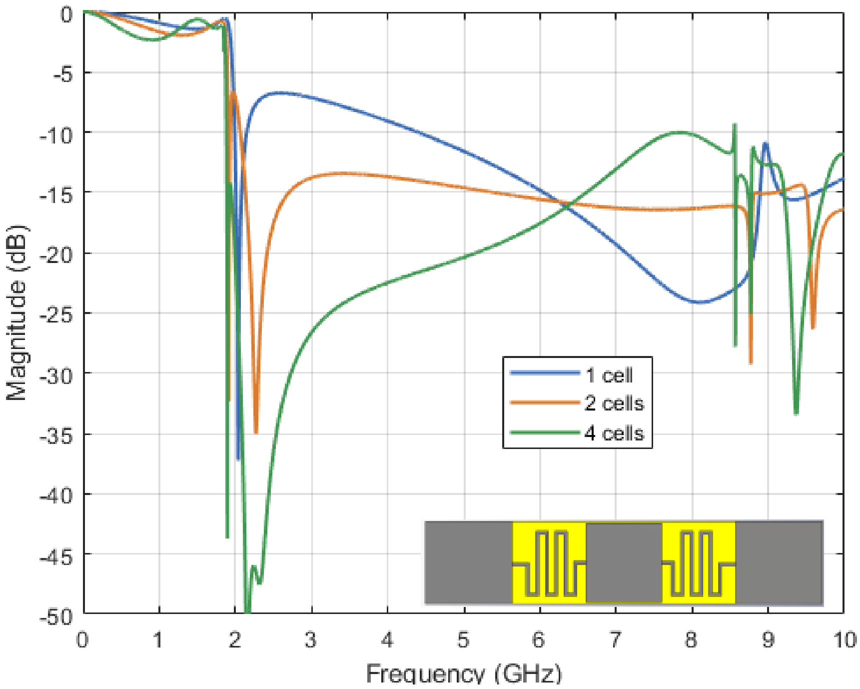

Figure 2.12. S_{21} parameter for the common mode for the structure descripted in Figures 2.4 and 2.5 for 1, 2 and 4 cells.

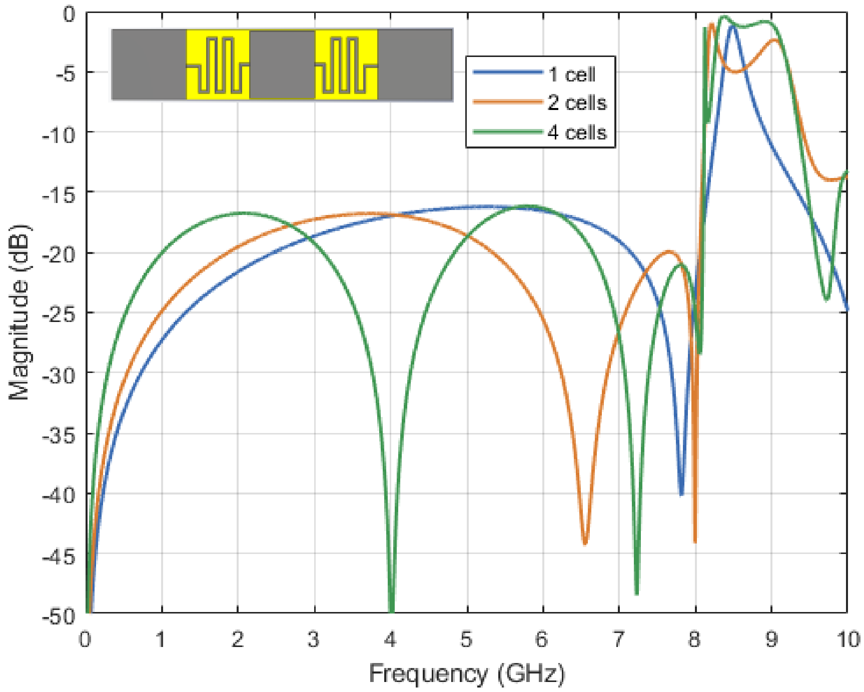

Figure 2.13. S_{11} parameter for the differential mode for the structure descripted in Figures 2.4 and 2.5 for 1, 2 and 4 cells.

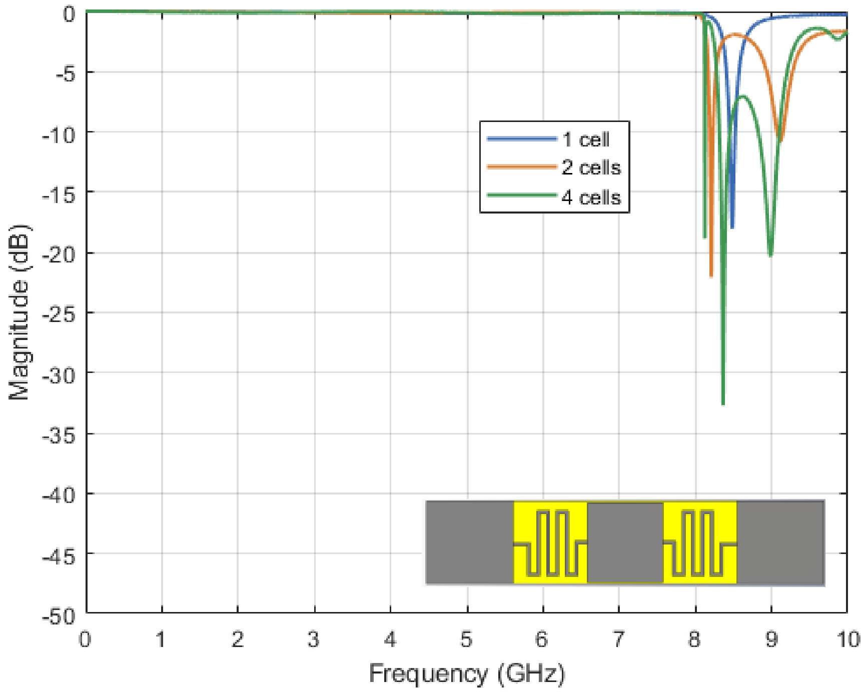

Figure 2.14. S_{21} parameter for the differential mode for the structure descripted in Figures 2.4 and 2.5 for 1, 2 and 4 cells.

From the results observed in the figures 2.11-2.14 we can ascertain the behavior of the filter. As mentioned before, this structure is a low pass-filter for the common mode, but for the differential mode it acts as an all-pass filter. The explanation behind this behavior will be explained further later, but as a first approximation we can say that this effect is induced by the presence of the meanders in the bottom plane.

Also, we observe the relationship between the number of unit cells in the structure and the final performance.

We can assert the following statements about the structure from the previous figures:

1. The structure with 1 cell should not be used since the attenuation at -10 dB starts much latter than the other two versions.
2. We can see that the bottom frequency of the filter (stated at -10 dB of attenuation) is almost the same for all versions, 1.9 GHz for the 4 cells version and 2 GHz for the 2 cells version.
3. The top frequency of the filter is fixed by the differential mode at 8.1 GHz for both versions, 2 and 4 cells. The common mode remains attenuated even at 10 GHz.
4. The main difference between the 4-cells and the 2-cells versions is that in the former, we achieve a bigger maximum attenuation than in the latter, but this attenuation is more stable in the 2-cells version. We can see how at 6.5 GHz the attenuation is bigger in the 2-cells version than in the 4-cells one.
5. We can also remark that the number of poles in the S_{21} parameter is related with the number of cells that are used.

In the table 2.2 we can observe better the ranges of interest for the different structures:

Structure / Mode	Common Mode		Differential Mode		Effective range	
	Range (GHz)	Related to 1 cell (%)	Range (GHz)	Related to 1 cell (%)	Range (GHz)	Related to 1 cell (%)
1 cell	4.4 – 10	-	0-8.44	-	4.4 – 8.44	-
2 cells	2 – 10	+ 42.8 %	0-8.12	- 3.8 %	2 – 8.12	+ 51.5 %
4 cells	1.9 – 10	+ 44.6 %	0-8.19	- 3%	1.9 – 8.19	+ 55.6 %

Table 2.2. Performance comparison.

As we can see in the table 2.2, we observe that the structure with one cell is not a good implementation in order to achieve the best results. Them, if we look at the 2 and the 4 cells versions, there is not a significant difference between them. As mentioned before, the 4 cells version has a bigger maximum attenuation while the 2 cells version has a more stable one.

In the figure we can see the dispersion diagram of this structure:

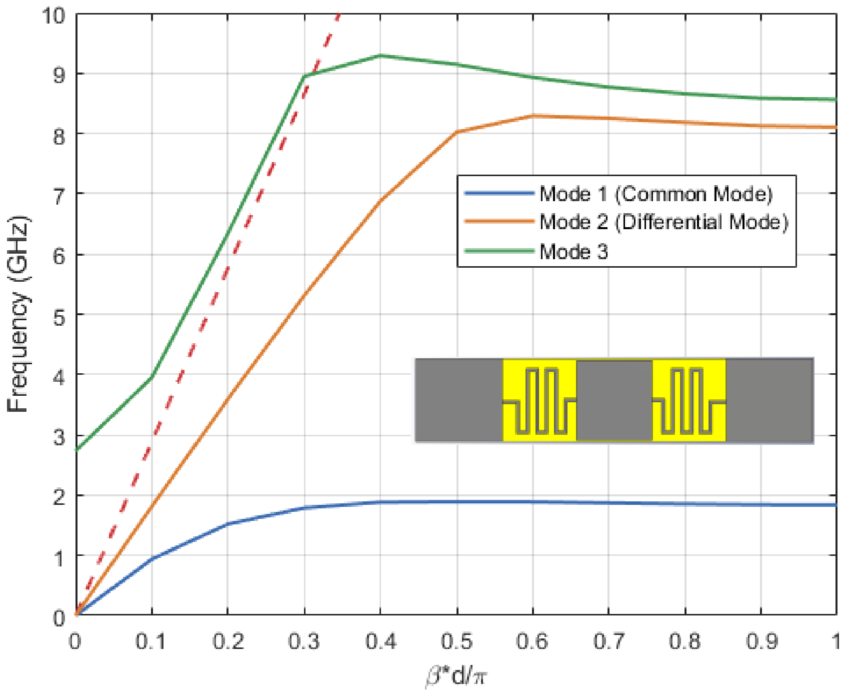

Figure 2.15. Dispersion diagram mode for the structure descripted in Figures 2.4 and 2.5.

We see how the results obtained from the dispersion diagram match perfectly with the ones showed in the S-parameters collected on the table. The effective bandwidth for this structure is from 1.9 GHz to 8.1 GHz. It's worth to remember that the dispersion diagram considers infinite number of unite cells, but we can see that these results match with the ones obtained for the 4 cells version. This means that we are not going to obtain any improvement using more than 4 cells.

2.3 Equivalent circuit analysis

In order to understand better the performance of the structure under the common mode we can model its behavior with an equivalent circuit made of lumped elements. The first step to do so is considering that under common-mode excitation we can assure that the structure will have a magnetic wall (even mode) in the symmetric plane so the current will be forced to flow partially through the meanders that we can observe between the patch and the ground plane, these are LC resonators.

The equivalent circuit that models the performance of the simulated structure can be observed in the figure 2.16.

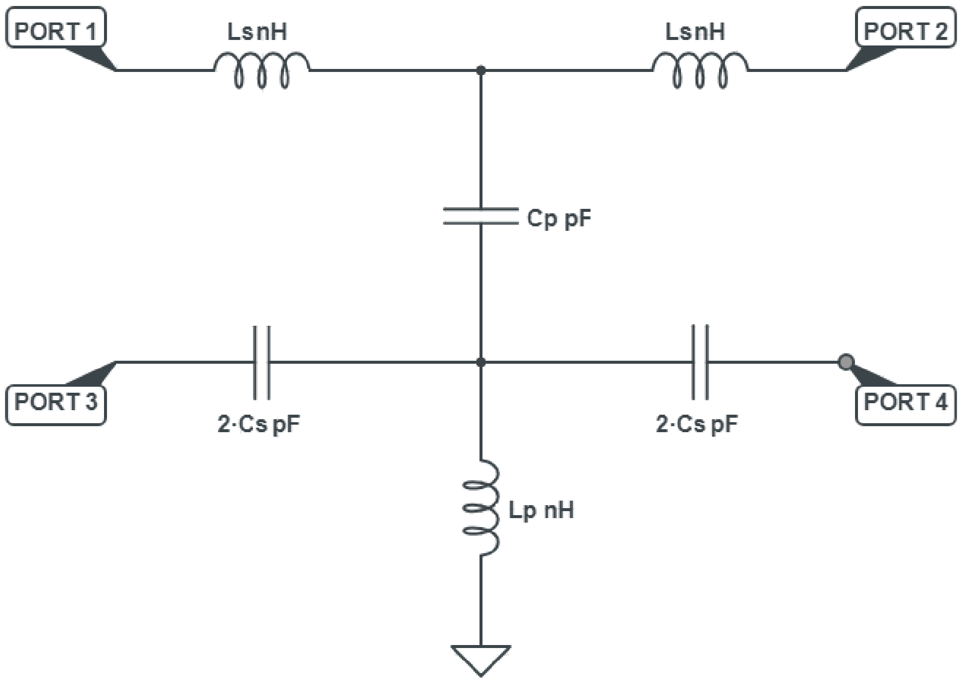

Figure 2.16. Equivalent circuit for the common mode.

The circuit is composed of two series inductances (L_s) and a shunt to the ground by the means of an inductance and a capacitance in series (L_p, C_p). The inductance, L_p, considers the inductance of the top side printed strips while the capacitance, C_p, accounts for the capacitive coupling between the top and bottom side metals. The two extra capacitors, C_s, take into account the electric coupling between the central patches of the bottom side. If the separation between patches is large enough, the contribution from these capacitors can be neglected, so the equivalent circuit would only be a low-pass 2-port network. In this case, where the capacitors can be neglected, the structure would reject common-mode signals above the resonant frequency of the meanders connected to ground plane. In the case of study, we have to take into account the influence of the defected ground structure (DGS) on common-mode operation.

In the figures 2.17-2.18 we can observe how the e-field propagates in the structure depending on the frequency.

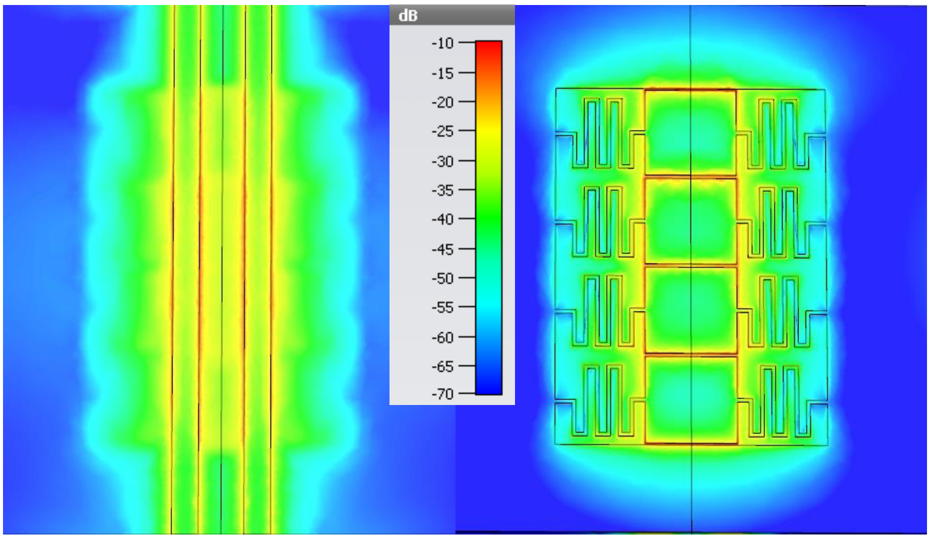

Figure 2.17. Average e-field at 1.5 GHz.

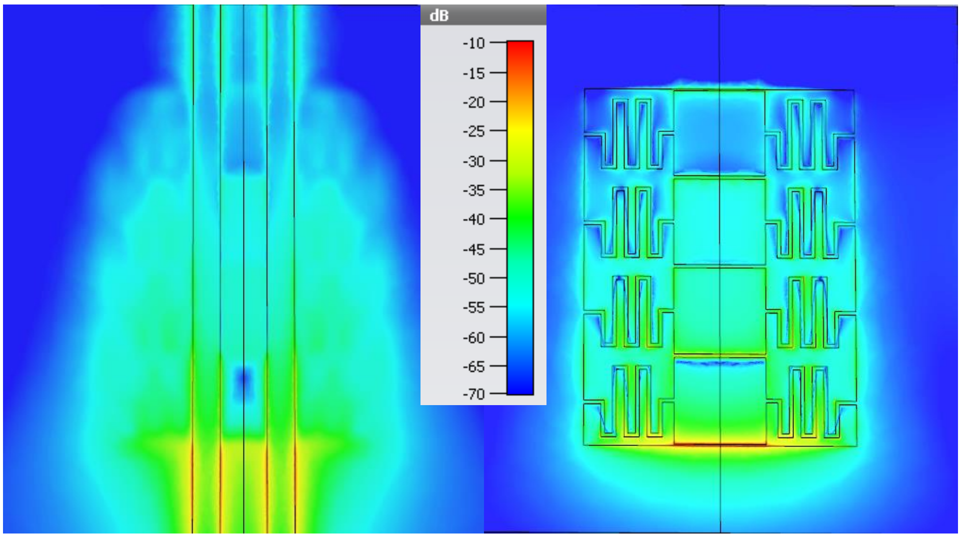

Figure 2.18. Average e-field at 5 GHz.

As we have seen with the S-Parameters the structure has its cutoff frequency at 2 GHz so in the figures 2.17-2.18 we can see how before that value the fields are able to pass all the way to the second port but when the frequency is over the cutoff frequency the energy is reflected to the first port or dissipated by the meanders to the ground plane, this way, there is almost no energy reaching the second port. We can also ascertain from these figures that, as we previously guessed from the S-parameters, that there is not really a great difference in the behavior of the filter when it has more than three unit cells, since the most part of the energy is dissipated on the first three stages of the filter. So, we think that the structure with four cells is the best option, more cells would not bring us better performance. This behavior could also be observed on the dispersion diagram, when we commented that four cells were the optimum case.

In the case of the differential mode the symmetric plane behaves as a perfect electric conductor (odd mode), so the return path for the current is only slightly affected by the ground plane modifications like we can see in the following figure, where we compare a regular double microstrip line of the same length of the 4 cells version with this structure.

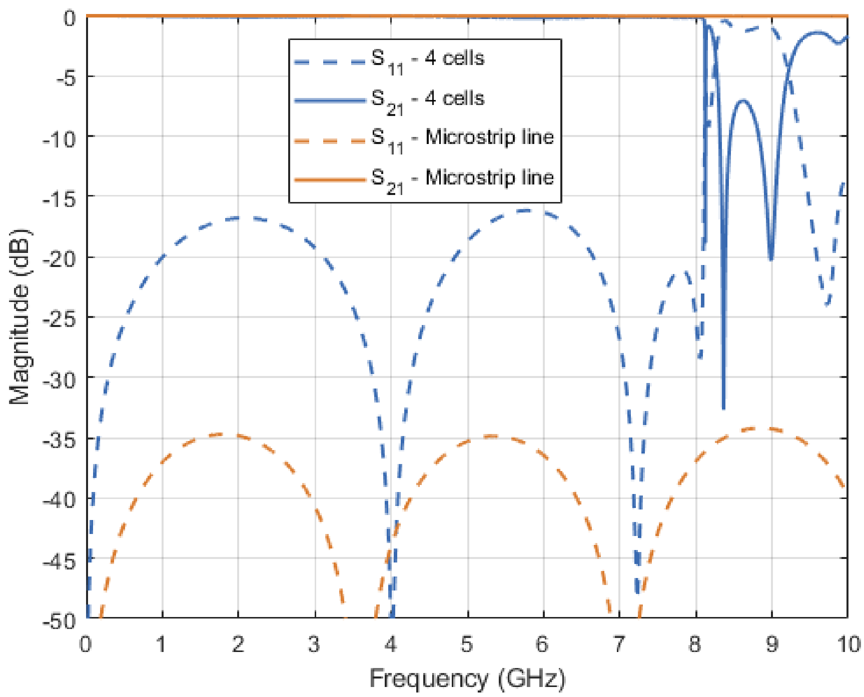

Figure 2.19. Comparison of S-Parameters between a regular microstrip line and the 4-cells structure for the differential mode.

In the figure 2.19 we observe how the structure under study behaves the same way as a regular microstrip line until 8.19 GHz. The only difference is the level of attenuation, but it's not an important matter since -16 dB is enough attenuation for communications and the overall behavior of the filter is the most important thing.

We can also demonstrate this behavior with the e-field representation. This way we can see that the current flowing through the high impedance meandered lines is practically negligible since these inductors are short-circuited at their two ends, to ground plane in one case and with the virtual PEC symmetric plane at the other.

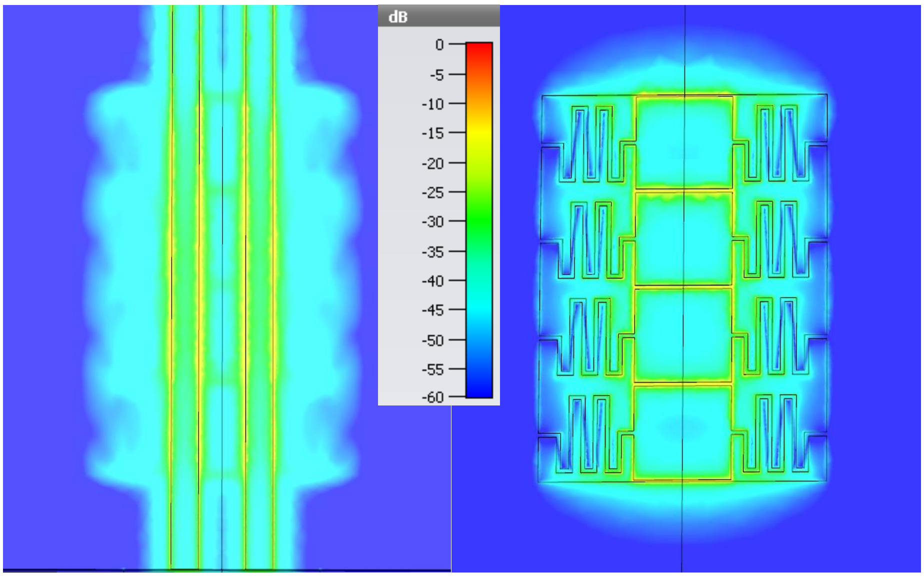

Figure 2.20. Average e-field at 5 GHz.

We observe in the figure 2.20 how the currents will flow mostly through the coupled lines, with only a small portion flowing over the rectangular patches and through the gaps between them. This way, as we have said before, the structure will behave as an all-pass filter under differential mode operation, with the characteristic impedance corresponding to the differential mode.

Chapter 3: Higher symmetries

3.1 Introduction to higher symmetries

At this point, we have a full understanding of the original structure; its behavior and performance have been clearly exposed and discussed to this point. So, now we are going to explain the modifications that this structure is going to experiment. The concept that we are going to apply is known as higher symmetries.

Firstly, before we start to explain this concept in detail, we will expose the different kind of fundamental symmetries that we can find inside the geometric symmetry.

1. Spherical symmetry. It's referred to a central point and happens when every point distanced a certain amount from this center is equivalent to another one with the same distance.

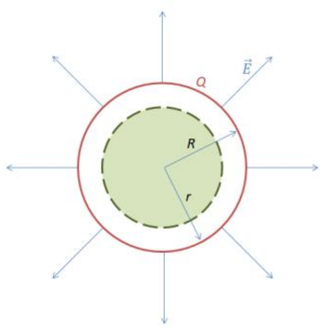

Figure 3.1. Spherical symmetry.

2. Axial symmetry. It's referred to an axis. An object is axially symmetric if its appearance is unchanged if rotated around an axis.

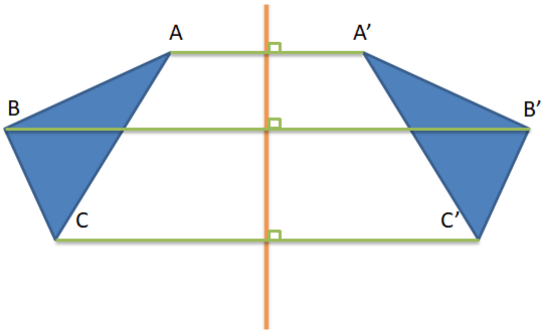

Figure 3.2. Axial symmetry

3. Reflective symmetry. Also known as mirror symmetry, happens if there is a line going through the object which divides it into two pieces which are mirror images of each other.

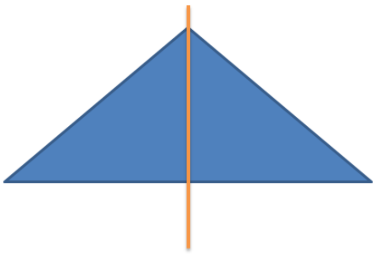

Figure 3.3. Reflective symmetry

4. Translational symmetry. An object has translational symmetry if it can be translated a certain amount, $T_a(x) = x + t$,without changing its overall shape.

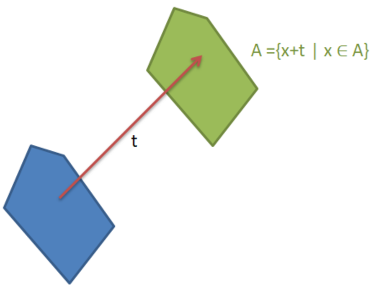

Figure 3.4. Translational symmetry.

The rest of symmetries can be viewed as a combination of the different kinds of symmetries mentioned before. In this context is where we encounter the higher symmetries. In this thesis, we are going to focus on glide symmetry, but we will also comment about twist symmetry since this is the other kind of higher symmetry that is being employed along with glide symmetry in the last years.

Also, it's worth mentioning that these higher symmetries are employed to create periodic structures in order to maximize the advantages of the effects that are related to its own implementation.

3.2 Glide Symmetry

3.2.1 Introduction

As mentioned before, the rest of symmetries can be explained from the fundamental symmetries. Glide symmetry, also known as transflection, is a kind of symmetry that involves two fundamentals, the translational and the reflection symmetries.

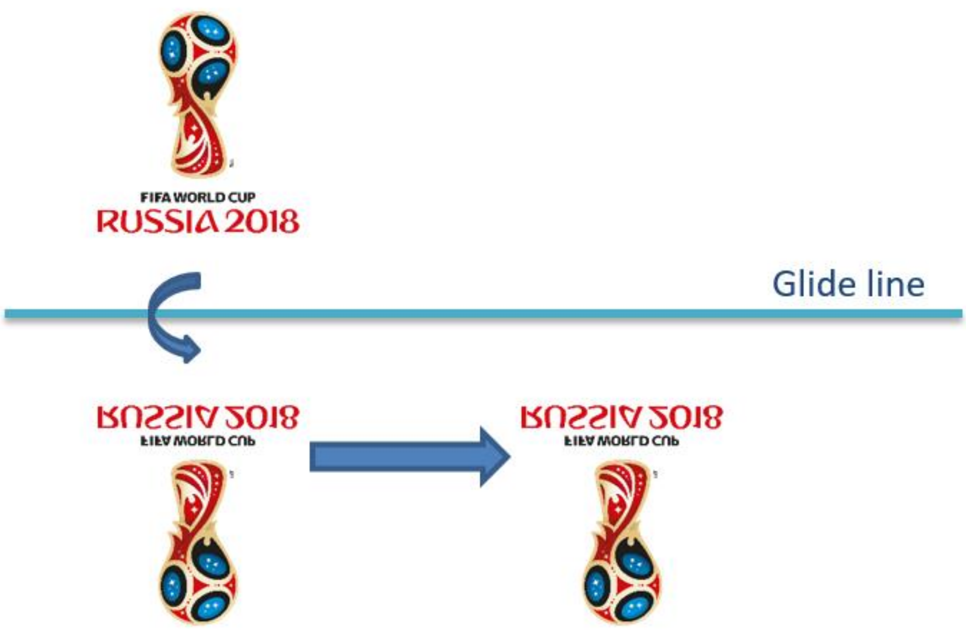

Figure 3.5. Glide symmetry.

If we consider a 2D problem where the reflection is in the x-axis and the translation is in the y axis, them, we can express the glide symmetry as:

$$(x, y) \rightarrow (x + t, -y)$$

3.2.2 Implications

The reason to explain why we are studying the effects of this kind of symmetry is motivated by the latest studies on this field that show a series of advantages with respect the original structures without increasing the cost or the complexity of the problem.

We can see on [8] how the employment of glide symmetry over a regular holey metasurface can produce a low dispersive equivalent refractive index that allow us to design ultrawideband planar lenses. We can also see that this glide symmetry results on a curve of the first mode almost straight over a wide range of frequencies, which means that the mode would be almost nondispersive [12-14].

Another advantage that comes with the implementation of glide symmetric structures is that they have been proved that are able to produce low-cost gap waveguide solutions as seen in [9, 15-17]. This is true since glide symmetry, as mentioned before, is just a combination of a mirroring and a translation of the original structure, so the resultant design is not more complex or expensive that the original one.

Finally, glide symmetry was also employed to reduce the dispersion of coplanar technology and propagation in slots, which can be employed to control the location of bandgaps, and to produce low-dispersive leaky-wave antennas [18,19].

3.3 Twist symmetry

3.3.1 Introduction

Twist symmetry is another kind of high-symmetry; this one only involves the translation and the spherical symmetries. These kinds of structures are created by a translation and angular rotation.

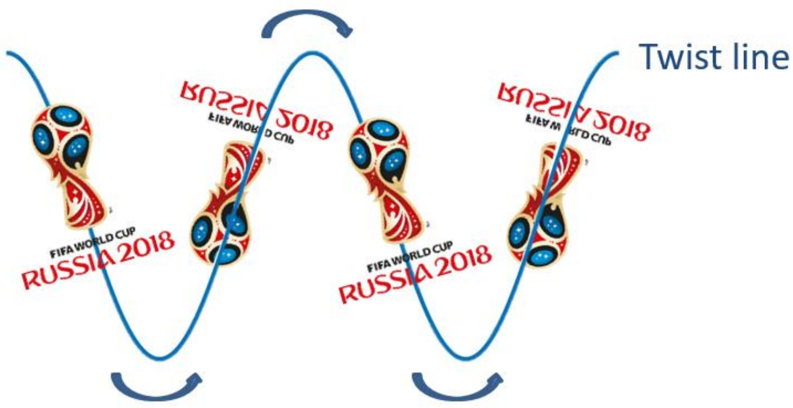

Figure 3.6. Twist symmetry.

In this case, we can express this symmetry as follows:

$$(x, y) \rightarrow (x + t, y + \theta)$$

3.3.2 Implications

Twist symmetry has been less studied than glide symmetry since the latter one is easier to implement into a wide range of previous structures that have been done employing regular axial symmetry, like in this work. Nevertheless, twist symmetry has been proved to be very useful when applied to coaxial cables, we can see in [9] how the implementation of twist symmetry can be used to reduce significantly the dispersion present in the conventional coaxial.

Chapter 4: Effects of applying glide symmetry over the original structure

Previously to this section we have shown the performance of the original structure in terms of S-parameters and dispersion diagram. Also, we have presented the higher symmetries that will serve us as basis to apply modifications to the structure. As we have mentioned before, we are going to employ glide symmetry and we will observe the changes introduced by this modifications over the structure.

If we observe the original structure and try to apply directly the glide symmetry, we will see that is not possible to obtain a full glide symmetric structure with a period of translation of half unit cell. This is because the gaps between patches in the bottom plane are situated in the position that should reside the meanders after the translation, this way, after applying glide symmetry the meanders wouldn't be in contact with the patches.

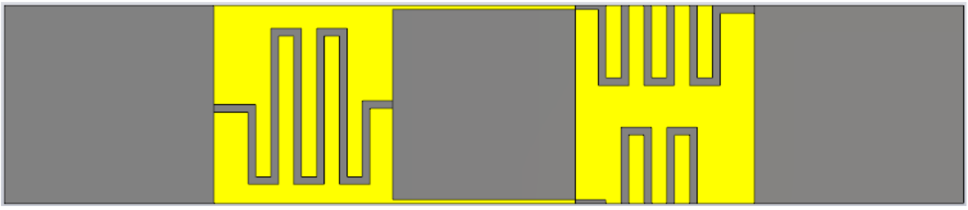

Figure 4.1. Glide symmetry with period equal to half unit cell.

As we can see, this new structure would be completely useless because of the lack of contact.

So now, in order to be able to study the effects of applying glide symmetry on the structure we need to slightly modify this structure, making the patch to occupy the full length of the unit cell.

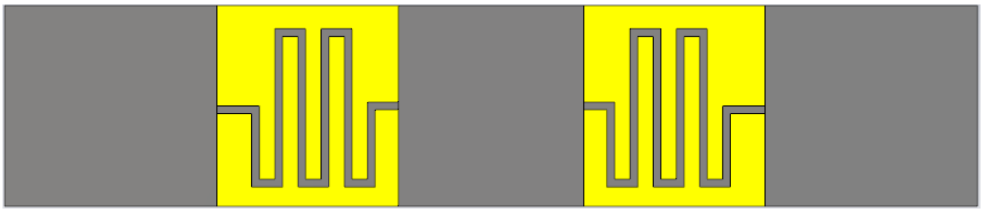

Figure 4.2. New structure with continuous line instead of patches.

For the purpose of keeping the patches we can also try to study a different approach of applying glide structure. After multiple tries we'd like to propose the following structure which can be considered glide. We'll talk about this structure afterwards.

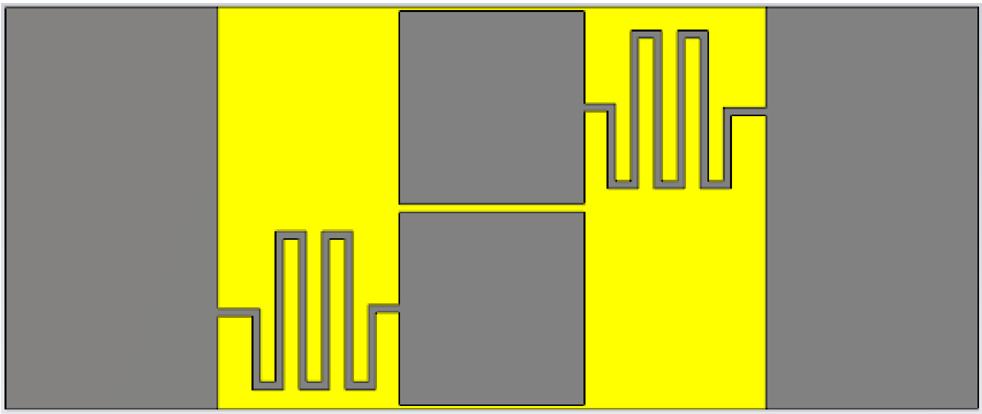

Figure 4.3. Another approach of applying glide symmetry.

We have also investigated the application of the glide symmetry on a different way. In this new structure, the reflection will be done in the z-axis, not in the y-axis like before; this way, the structure will have three layers, instead of the previous two.

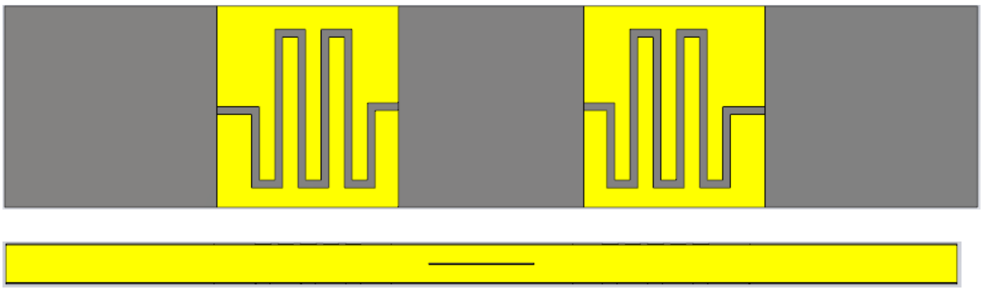

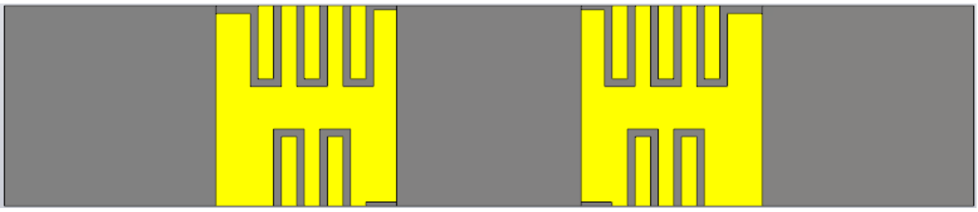

Figure 4.4. Glide symmetry of 3-layers new structure and period equal to half unit cell (Top, side and bottom view).

It has to be noted that we have removed one of the two striplines, keeping the other one in the center with a new width of two times the previous one. This change is made on these new structures of study because of two reasons. Firstly, we only want to study the common mode since is the mode of interest for us since it is the only one that will be affected by the introduction of glide symmetry. And in second place, this way, the manufacture process will be easier since it is more difficult to do the feeding of a differential line than of a single line. Finally, the new width of two times the previous one is not arbitray, it has been done this way to keep the capacitance between the top and the bottom plane the same, so we do not introduce changes in the behavior.

So, in the following subsections we will present the results obtained for these new structures. We will group them in a way that let us obtain a better view of the effect of applying glide symmetry.

4.1 2-layers structures without patches

In this subsection we will focus on three structures related to the new structure without patches that we have mentioned before. In this case we are going to study the modified original structure, its glide structure, and another structure with a shift of a quarter of cell. This last structure cannot be considered glide but it is worth studying the effects that come from the use of an intermediate structure.

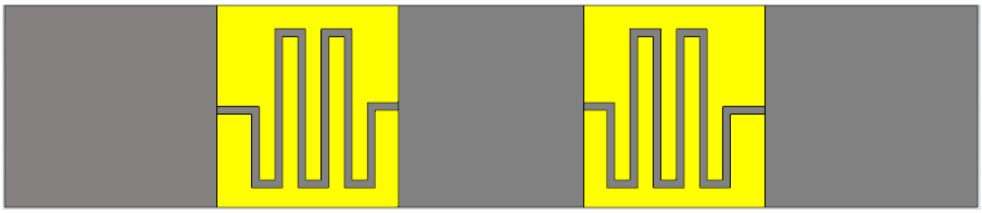

a)

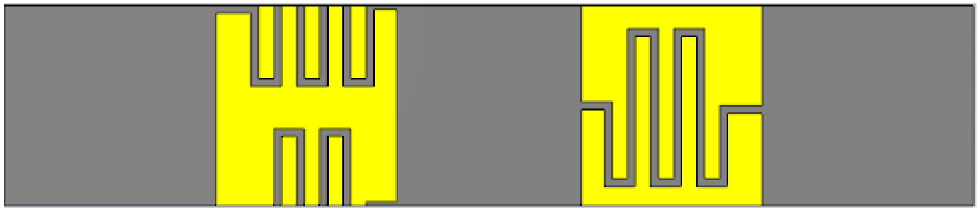

b)

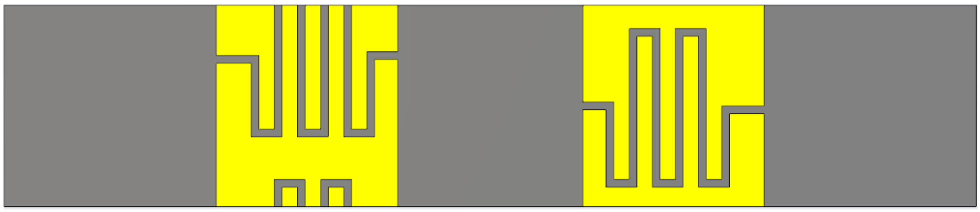

c)

Figure 4.5. Unit cells of the structures under study: a) Original structure without patches. b) Structure with glide symmetry. c) Structure shifted a quarter of cell.

Then, we will compare the S_{21} parameter from these structures, so we can have a quick and good understanding of the effects introduced by the glide symmetry. The S_{21} parameter will be the parameter we will use to compare the different structures since it is the most interesting one for filters.

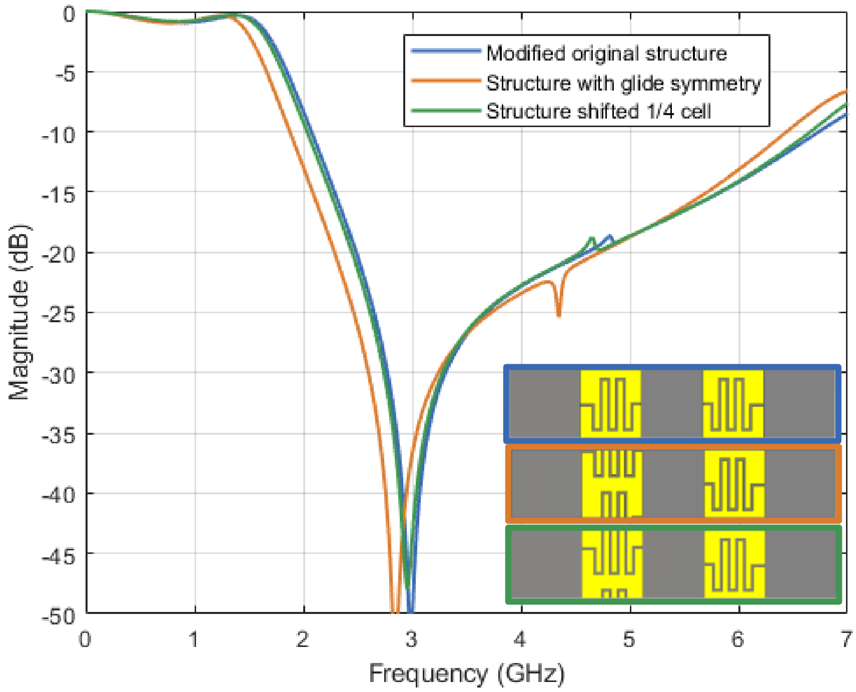

Figure 4.6. S_{21} parameter for the structures under study descripted in the figure 4.5.a (blue), 4.5.b (orange) and 4.5.c (green).

In the figure 4.6 we clearly observe some changes in the behavior of the filter. In the first place, if we compare this new behavior with the one observed in the original structure we can see that the number of poles is reduced to one, this is because we have removed the patches that introduced the poles before, this way, in this structure will be easier for us to see the differences in the behavior.

Now, if we compare the results obtained we can see that the shift of a quarter of cell does not really affect the bandwidth of the filter, it just shifts downwards the frequency 40 MHz, so this kind of structure does not have a big impact on the original structure.

In the other hand, when we apply glide symmetry we observe how the band of operation of the filter is shifted downwards 200 MHz. This is a nice performance since we are keeping the same number of elements and dimensions to achieve a filter that operates in lower frequencies.

4.2 3-layers structures without patches

In this subsection we will study the effects of applying a third layer to the structure, this way, we are going to have something similar to a stripline structure with a deformed ground plane. Here, we are going to study 3 structures, a z-symmetric case of the modified original structure and two glide cases, the first one will be achieved by doing the reflection over this symmetric structure in the y-axis and the translation in the x-axis, and the second one will be achieved by using the z-axis as the mirror plane for the reflection over the modified original structure and the x-axis as the shift plane for the translation.

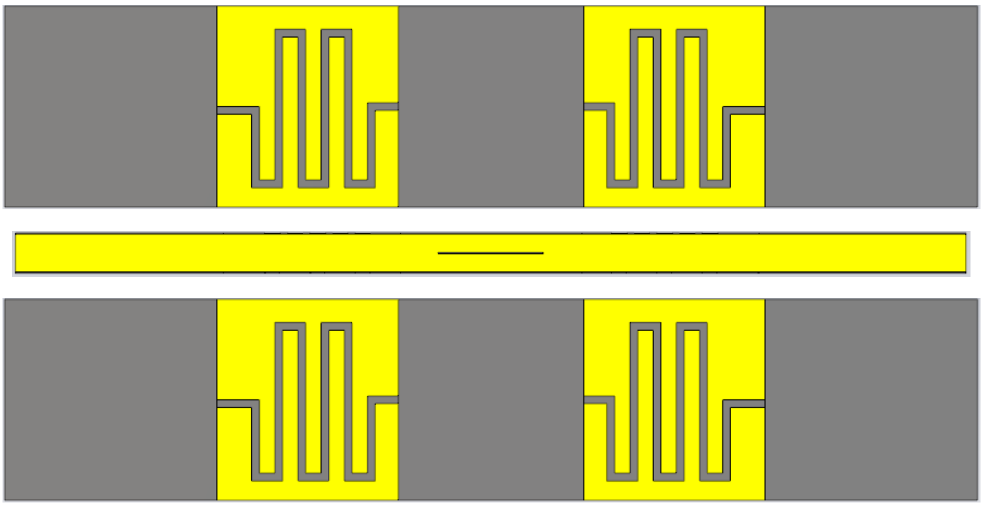

a)

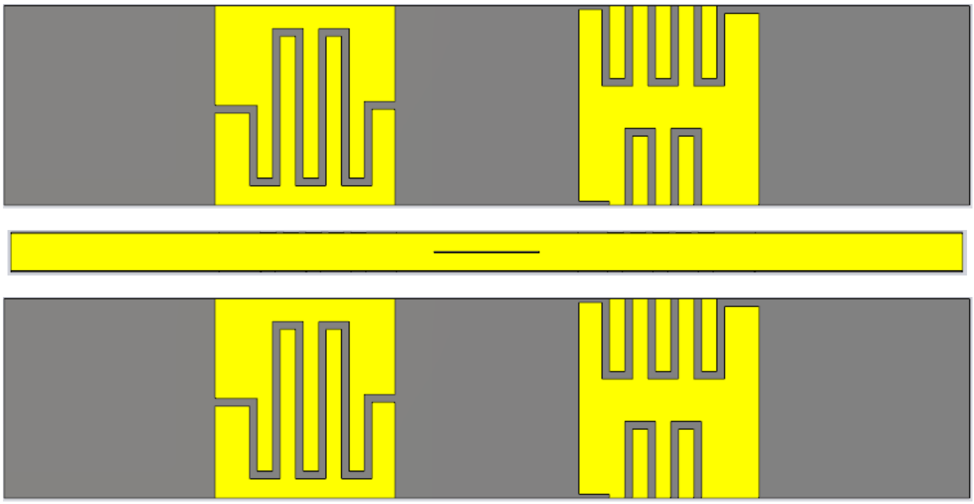

b)

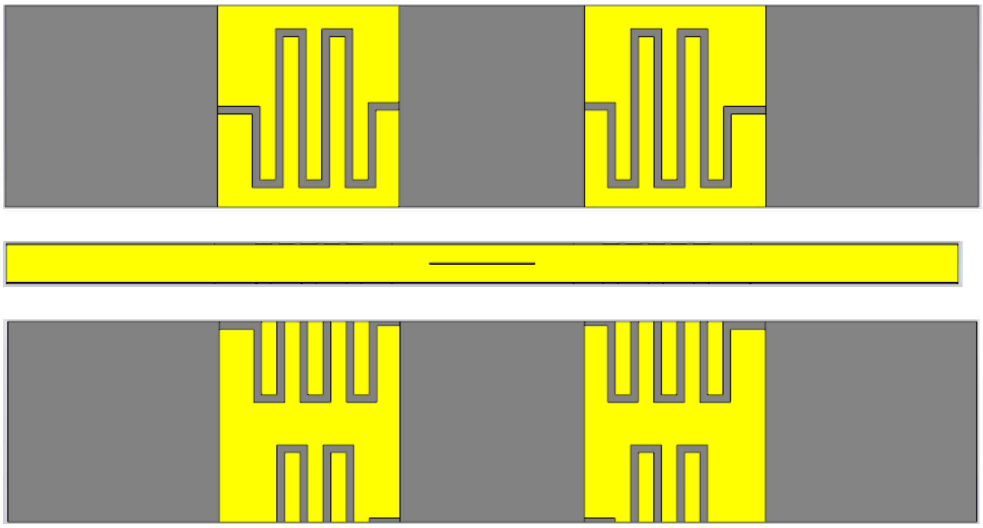

c)

Figure 4.7. Unit cells of the structures under study: a) z-symmetric structure. b) Structure with glide symmetry over y-axis. c) Structure with glide symmetry over z-axis.

Again, we are going to study the S_{21} parameter in order to observe the changes introduced by the glide symmetry.

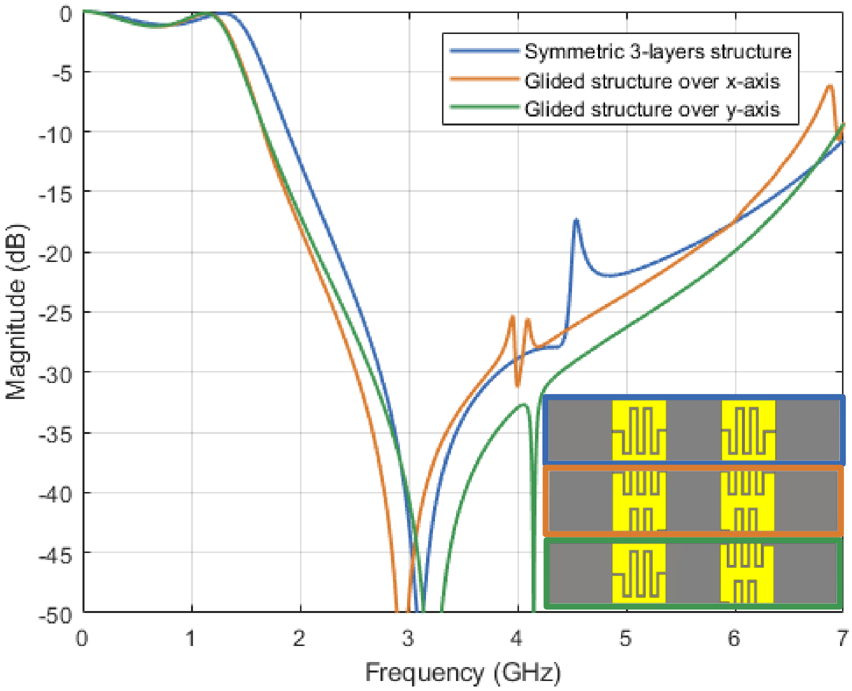

Figure 4.8. S_{21} parameter for the structures under study descripted in the figure 4.7.a (blue), 4.7.b (green) and 4.7.c (orange).

The results obtained in the figure 4.8 let us compare two different ways of applying glide. We observe that both ways of applying glide symmetry shift the frequency downwards like we observed in the previous case. Nevertheless, when we apply glide over the y-axis the results are better since we are not only shifting the frequency downwards 250 MHz, but we also manage to reduce the decrease of the bandwidth of the filter, the glided symmetry described in figure 4.7.b has a bandwidth 300 Mhz bigger than the one described in figure 4.7.c. The overall attenuation is also increased in 3 dB on the glided structure showed in figure 4.7.b.

4.3 Glide symmetry over 2-cells structure

In this section we are going to focus on the case which we mentioned previously that had 2-cells as unit cell. This is a weird case of glide symmetry that we came up with whose performance is superb as we will see next. For reference we are going to use the 4-cells original structure and we also are going to use the figure 4.9.b as reference in order to study another structure with the same number of elements as the glided one.

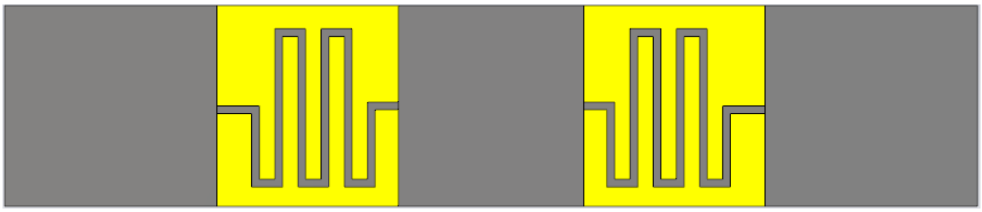

a)

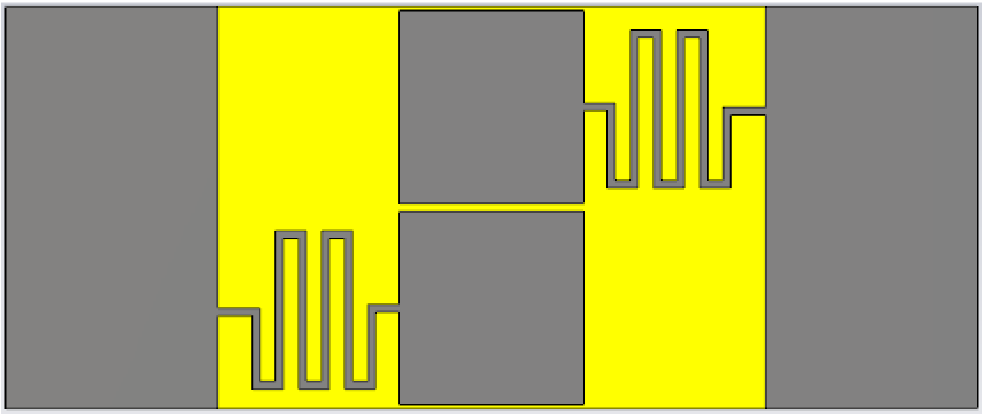

b)

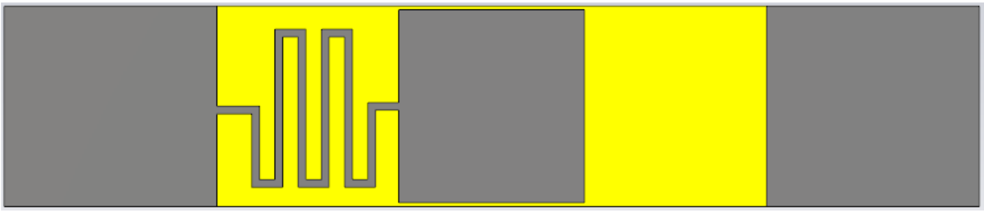

c)

Figure 4.9. Unit cells of the structures under study: a) Original structure. b) Structure with interleaved meanders. c) Structure with meanders on one side.

The S_{21} parameter related to these structures is represented in the figure 4.10.

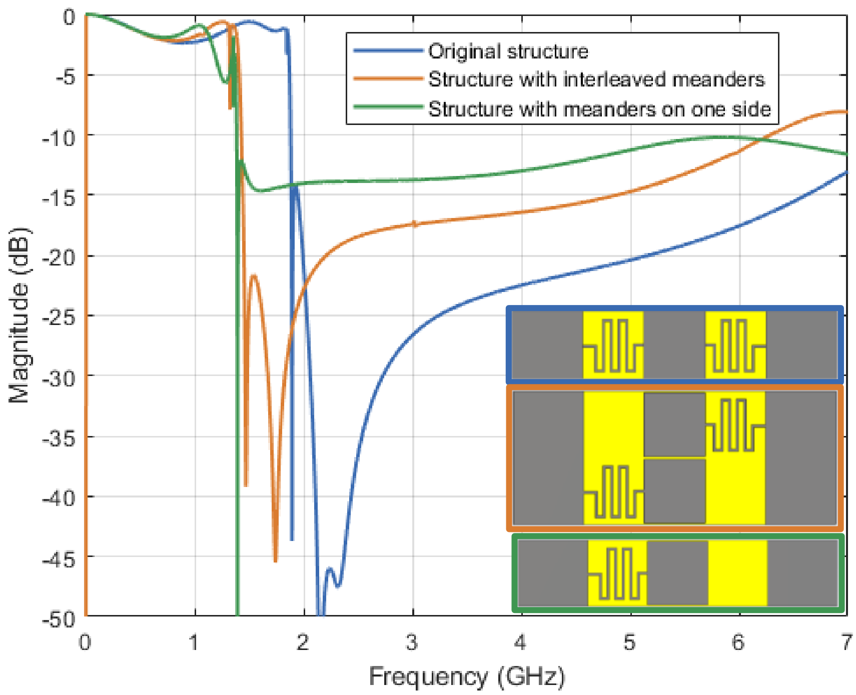

Figure 4.10. S_{21} parameter for the structures under study descripted in the figure 4.5.a (blue), 4.5.b (orange) and 4.5.c (green).

As we have mentioned before, the results that we have obtained with this new structure are very good. Not only because we have been able to shift the frequency 460 MHz downwards but also because we have used less elements than in the original case, in this new structure we make use of 4 meanders instead of the 8 meanders presented in the original structure.

This behavior is not only presented in the structure with interleaved meanders, but also in the one with the four meanders in one side. Nevertheless, the glided structure has an overall bigger attenuation than the one with the meanders on one side.

We have to say that this behavior has come as a surprise as we didn't expect such good results from these modifications to the original structure since we are reducing the amount of metal, reducing the inductance, and increasing the separation between meanders, also reducing the capacitance.

Chapter 5: Prototypes

Three prototypes have been manufactured in order to validate the results. These prototypes belong to the 2-layers group. In the figures 5.1 and 5.2 we observe these structures.

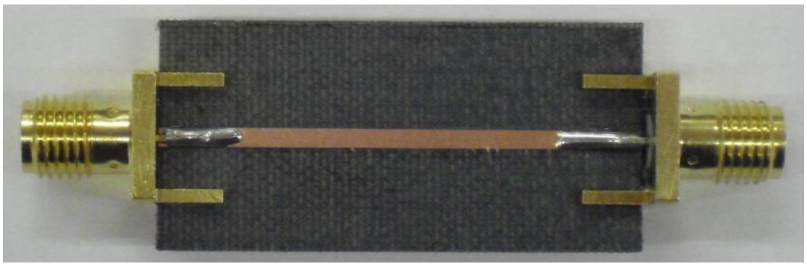

Figure 5.1 Common top view for the three manufactured prototypes.

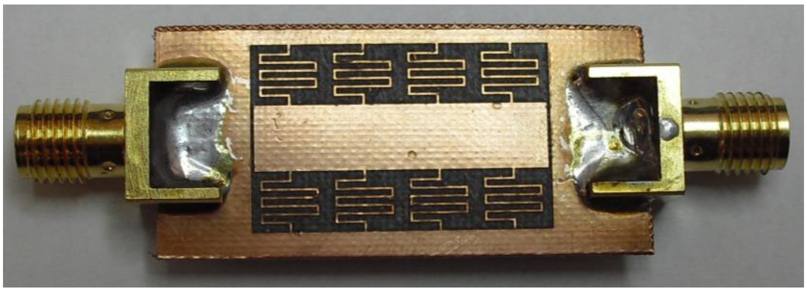

a)

b)

c)

Figure 5.2. Bottom view for the three manufactured prototypes: a) Modified structure without patches; b) Structure with glide symmetry keeping the number of elements; c) Structure with glide symmetry keeping the original length of the filter.

The first of the structures, depicted in figure 5.2.a, represents the original structure with the continuous line in the ground plane, this will serve as reference to test the results from the glide structures depicted in 5.2.b and 5.2.c. The difference between these two glided structures is that in the first one we have applied glide symmetry over all the structure, this way the length of the resultant filter is bigger than in the original one. So, in order to keep the same length, a third prototype has been manufactured removing one meander but keeping the glide symmetry.

In the figure 5.3 we have represented the results obtained by both, the simulations and the measurements of these structures.

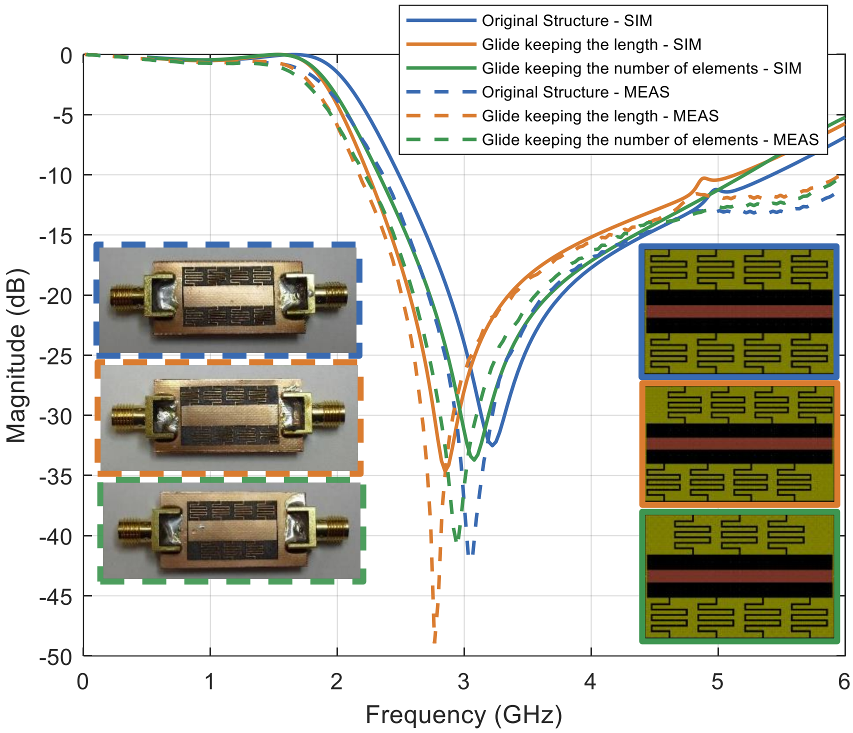

Figure 5.3. S_{21} parameter for the simulated and measured structures depicted in figures 5.1 and 5.2

The prototypes measured have experimented a little shift in the frequency with respect the simulated results, nevertheless, this shift is between the tolerance range and may be due to little changes on the dielectric constant of the substrate or to manufacture issues, since this is a design that requires precision since the dimensions are very small.

These results let us validate the phenomenon studied in this thesis. The frequency has been shifted downwards with respect the original design. The characteristics of the two glided designs manufactured are very similar, nevertheless the design that keeps the length has suffered a stronger downwards shift in the frequency that the one that keeps the elements, 200 MHz for the case that keeps the length instead of the 150 MHz of the case that keeps the number of elements.

Chapter 6: Sustainability

We have already mentioned that this kind of filter is best used for wireless communications or new technologies such as Internet of Things due to the inherent behavior of the filter that can be employed as a pre-stage to remove the common mode for the overall system.

Internet of Things is a newly adapted concept that means that a lot of devices will be connected between each other and with Internet. The number of sensors and devices that will be connected is expected to be enormous, more than trillions of devices will be used only on this technology.

This way we can expect that the question about the environmental impact is going to be asked. Printed circuit boards (PCB) such as the ones we have designed and studied in this thesis are under vigilance because of this matter, since PCBs are the basis of high quality electronics products, not only in IoT but also in a daily basis.

In this section, we will explain the impact that has this kind of circuitry over the environment. It has to be mentioned that we will focus on the general impact of complete systems or devices manufactured that make use of PCBs, since this thesis is only focused in a small part of those systems, the filters, so we cannot isolate this particular impact inside the full systems.

PCBs are generally composed of Small Outline Integrated Circuits (SOIC), Plastic Leaded Chip Carrier (PLCC), chip components, lumped elements, metallic lines, solders... So, when trying to explain the impact of PCBs over the environment, we cannot focus on only one component.

One of the main problems that are presented is the low recycling rates of electronic devices, in the last 20 years the increase of electronic devices in our daily routine has increased exponentially and many of those devices are not correctly recycled after their useful life. The generation rate of waste electric and electronic equipment (WEEE) is always increasing. According to data retrieved from the European Commission [11], from the 9 million tonnes generated in 2005, it's expected to grow to more than 12 million tonnes by 2020. WEEE is a complex mixture of materials and components that because of their hazardous content, and if not properly managed, can cause major environmental and health problems. WEEE doesn't only include PCBs but PCBs don't usually work alone, in almost every electronic equipment we can see PCBs along with other devices, so we cannot isolate this because it wouldn't be real.

For the Europe Commission, this is a very important issue that must be addressed. Two pieces of legislation have been put in place: The Directive on waste electrical and electronic equipment (WEEE Directive) and the Directive on the restriction of the use of certain hazardous substances in electrical and electronic equipment (RoHS Directive).

The first WEEE Directive (Directive 2002/96/EC) was released in February 2003. This Directive provided for the creation of collection schemes where consumers return their WEEE free of charge. These schemes aim to increase the recycling of WEEE and/or re-use.

This Directive was proposed to be revised in December 2008, after the non-stop increase of waste stream. The new WEEE Directive 2012/19/EU entered into force on 13 August 2012 and became effective on 14 February 2014.

EU legislation restricting the use of hazardous substances in electrical and electronic equipment (RoHS Directive 2002/95/EC) was released in February 2003. The legislation requires heavy metals such as lead, mercury, cadmium, and hexavalent chromium and flame retardants such as polybrominated biphenyls (PBB) or polybrominated diphenyl ethers (PBDE) to be substituted by safer alternatives. In December 2008, the European Commission proposed to revise the Directive. The RoHS recast Directive 2011/65/EU became effective on 3 January 2013.

Chapter 7: Conclusion and Future Lines of Research

This master thesis has allowed us to investigate the outcomes of applying glide symmetry to a mature technology such as microstrip technology, which was thought to be fully developed without room for improvement.

We have proved that the implementation of this kind of symmetry is worth it since without making the structure more complex we achieve a better behavior in lower frequencies. This is a significant fact since it tends to be more difficult to obtain better results in the lower frequencies than in the higher ones. Also, this behavior let us manufacture filters at lower frequencies without having to increase the dimensions, which is a very important advantage that comes from the results obtained in this thesis.

In this thesis we have studied the application of the glide symmetry in different ways, we have seen the phenomenology that comes from its implementation, which as mentioned before, is very interesting. Therefore, at this point we think that the immediate future line of research would be to focus on the theory or explanation behind these phenomena. We can offer some conjectures about this, but further work is required in order to offer a good explanation.

Glide symmetry is a new research field, and this offer us the possibility to investigate its repercussion in many different ways that have not been explored before, such as the one we have addressed in this thesis. Furthermore, from the results obtained on this thesis and the ones reviewed in other works we can assert that this is a subject that is worth studying.

References

[1] A. Fernández-Prieto, J. Martel, F.Medina, F.Mesa, Shilong Qian, Jia-Sheng Hong, J. Naqui and F. Martín, “Dual-band differential filter using broadband common-mode rejection artificial transmission line,” Progress In Electromagnetic Research, Vol. 139, 779-797, 2013.

[2] C. Pinkle, “The Why and How of Differential Signaling,” Retrieved from https://www.allaboutcircuits.com/technical-articles/the-why-and-how-of-differential-signaling/

[3] S. Sattel, “What Is Differential Signaling?” Retrieved from https://www.autodesk.com/products/eagle/blog/what-is-differential-signaling/

[4] Tseng, B.-C. and L.-K. Wu, “Design of miniaturized commonmode filter by multilayer low-temperature co-fired ceramic,” IEEE Trans. Electromagn. Compat., Vol. 46, No. 4, 471–579, November 2014.

[5] Liu, W.-T., C.-H. Tsai, T.-W. Han, and T.-L. Wu, “An embedded common-mode suppression filter for GHz differential signals using periodic defected ground plane,” IEEE Microw. Wireless Compon. Lett., Vol. 18, No. 4, 248–250, April 2008.

[6] Wu, S.-J., C.-H. Tsai, T.-L. Wu, and T. Itoh, “A novel wideband common-mode suppression filter for gigahertz differential signals using coupled patterned ground structure,” IEEE Trans. Microw. Theory Tech., Vol. 57, No. 4, 848–855, April 2009.

[7] J. Naqui, A. Fernández-Prieto, M. Durán-Sindreu, F. Mesa, J. Martel, F. Medina, and F. Martín, “Common mode suppression in microstrip differential lines by means of

complementary split ring resonators: Theory and applications,” IEEE Trans. Microw. Theory Tech., Vol. 60, No. 10, 3023–3034, October 2012.

[8] O. Quevedo-Teruel, M. Ebrahimpouri and M. Ng Mou Kehn, "Ultrawideband Metasurface Lenses Based on OffShifted Opposite Layers," in IEEE Antennas and Wireless Propagation Letters, vol. 15, pp. 484-487, December 2016.

[9] M. Ebrahimpouri, O. Quevedo-Teruel, E. Rajo-Iglesias, “Design Guidelines for Gap Waveguide Technology Based on Glide-Symmetric Holey Structures”, IEEE Microwave and Wireless Component Letters, vol. 27, issue 6, 2017.

[10] O. Dahlberg, R. C. Mitchell-Thomas, O. Quevedo-Teruel, “Reducing the Dispersion of Periodic Structures with Twist and Polar Glide Symmetries”, Scientific Reports, vol. 7, article number 10136, 2017.

[11] Europe Commission about WEEE. Retrieved from http://ec.europa.eu/environment/waste/weee/index_en.htm

[12] G. Valerio, Z. Sipus, A. Grbic, O. Quevedo-Teruel, “Accurate equivalent-circuit descriptions of thin glide-symmetric corrugated metasurfaces”, IEEE Transactions on Antennas and Propagation, vol. 65, no. 5, pp. 2695-2700, May 2017.

[13] F. Ghasemifard, M. Norgren, O. Quevedo-Teruel, "Dispersion Analysis of 2-D Glide-Symmetric Corrugated Metasurfaces Using Mode-Matching Technique”, IEEE Microwave and Wireless Components Letters, vol. 28, no. 1, pp. 1-3, January 2018.

[14] G. Valerio, F. Ghasemifard, Z. Sipus, O. Quevedo-Teruel, “Glide-Symmetric All-Metal Holey Metasurfaces for Low-Dispersive Artificial Materials: Modelling and Properties", IEEE Transactions on Microwave Theory and Techniques, 2018.

[15] M. Ebrahimpouri, E. Rajo-Iglesias, Z. Sipus, O. Quevedo-Teruel, "Cost-Effective Gap Waveguide Technology Based on Glide-Symmetric Holey EBG Structures”, IEEE Transactions on Microwave Theory and Techniques, vol. 66, no. 2, pp. 927-934, February 2018.

[16] M. Ebrahimpouri, A. Algaba-Brazalez, L. Manholm, O. Quevedo-Teruel, "Using Glide-symmetric Holes to Reduce Leakage between Waveguide Flanges", IEEE Microwave and Wireless Components Letters, 2018.

[17] E. Rajo-Iglesias, M. Ebrahimpouri, O. Quevedo-Teruel, "Wideband phase shifter in groove gap waveguide technology implemented with glide-symmetric holey EBG", IEEE Microwave and Wireless Components Letters, 2018.

[18] M. Camacho, R. Mitchell-Thomas, A. P. Hibbins, J. R. Sambles, O. Quevedo-Teruel, "Mimicking glide symmetry dispersion with coupled slot metasurfaces", Applied Physics Letters, vol. 111, no. 12, p. 121603, 2017.

[19] M. Camacho, R. C. Mitchell-Thomas, A. P. Hibbins, J. R. Sambles, O. Quevedo-Teruel, "Designer surface plasmon dispersion on a one-dimensional periodic slot metasurface with glide symmetry", Optics Letters, Vol. 42, No. 17, pp: 3375-3378, 2017.

TRITA TRITA-EECS-EX-2018:492
ISSN 1653-5146